Nanoscience and Nanotechnology Letters
Vol. 9, 50–55, 2017

Photocatalytic Effect of Ag/TiO_2 Nanotubes Fabricated Using 40 nm-Scale BCP Lithography

Da In Sung[1], Hyun Gu Kim[3], Seung Keun Cha[4], Dong Hyun Kim[5], Han-Bo-Ram Lee[3], Sang Ouk Kim[4], Dong Woo Kim[1,*], and Geun Young Yeom[1,2,*]

[1] *School of Advanced Materials Science and Engineering, Sungkyunkwan University, 2066, Seobu-ro, Suwon, 16419, South Korea*
[2] *SKKU Advanced Institute of Nano Technology (SAINT), Sungkyunkwan University, 2066, Seobu-ro, Suwon, 16419, South Korea*
[3] *Department of Materials Science and Engineering, Incheon National University, 119, Academy-ro, Yeonsu-gu, Incheon, 22012, Republic of Korea*
[4] *National Creative Research Initiative Center for Multi-Dimensional Directed Nanoscale Assembly, Department of Materials Science and Engineering, KAIST, Daejeon, 34141, Republic of Korea*
[5] *Korea Institute of Ceramic Engineering and Technology (KICET), 101, Soho-ro, Jinju, 52851, Republic of Korea*

Uniform TiO_2 nanotubes were fabricated using a self-aligned, hole patterned BCP template lithography, atomic layer deposition of TiO_2, and reactive ion etching. Also, Ag nanoparticles were deposited onto TiO_2 nanotubes using a photochemical deposition method. Using the TiO_2 nanotubes deposited with and without Ag nanoparticles, the effect of TiO_2 nanotubes and Ag nanoparticles on the photocatalytic degradation was investigated by measuring the concentration change of the methylene blue solution under a UV light irradiation. Anatase phase TiO_2 nanotubes with 50∼60 nm height and 40∼50 nm diameter could be successfully fabricated and Ag nanoparticles with 7∼9 nm size could be also formed on the TiO_2 nanotubes. The use of TiO_2 nanotubes instead of flat TiO_2 film improved the photocatalytic effect due to the increased TiO_2 surface area and also the use of Ag nanoparticles on TiO_2 nanotubes further improved the photocatalytic effect up to 8% by slowing down the rate of electrons and holes recombination on the surface of TiO_2. However, when the coverage of Ag nanoparticles on TiO_2 nanotubes are too high, possibly due to the decreased UV penetration to TiO_2 by the increased surface area covered with Ag nanoparticles, the photocatalytic effect was decreased.

Keywords: TiO_2 Nanotubes, Environmental Photocatalysts, Ag Nanoparticles, Reactive Ion Etching.

1. INTRODUCTION

Titanium dioxide (TiO_2) is one of the multipurpose materials used for various functional applications such as solar cells, antibacterial agents, and photocatalysts for degradation of environmental contaminants due to its unique properties.[1–7] Especially, the environmental decontamination by nanosize TiO_2 photocatalysis is investigated to be appealing because of its low cost, nontoxicity, high surface-to-volume ratios, high surface activity, and simple recycling.[8,9]

The brief mechanism of the TiO_2 photocatalytic process is summarized in Figure 1.[10–12] When TiO_2 in an aqueous dye solution is irradiated with UV or sun light, where the energy is greater than its band gap energy, two types of carriers, electrons and holes, are photogenerated and separated. The generated electrons from the valance band to the conduction band can react with O_2 or acceptor molecule A. The reacted O_2 can be reduced to superoxide anion $O_2^{-\cdot}$ and acceptor molecule can be reduced $A^{-\cdot}$. The separated holes oxidize water or OH^- to produce $OH^\cdot$ radicals through a one-electron oxidation step. The OH free radicals and the superoxide anions degrade the dye compounds.

*Authors to whom correspondence should be addressed.

 1941-4900/2017/9/050/006 doi:10.1166/nnl.2017.2295

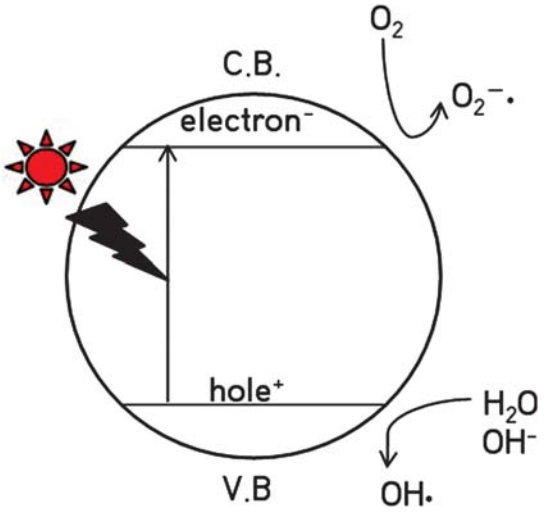

Fig. 1. Brief mechanism of the photocatalytic process of TiO_2.

Typically, two structured TiO_2 are being used, rutile and anatase.[1, 2, 4, 13, 14] Despite having the same chemical composition, due to the different chemical bonding of rutile and anatase structured TiO_2, they have different band gap energies of 3.03 eV and 3.20 eV, respectively. Anatase structured TiO_2 exhibits a significantly higher photocatalytic activity than rutile structured TiO_2 because of the higher charge-carrier mobility of 80 $cm^2/V \cdot s$ for anatase TiO_2, which is about 89 times faster than that of rutile TiO_2. Thus, anatase TiO_2 has better photocatalytic properties than rutile TiO_2. Also, at bulk phase, rutile TiO_2 is more stable while anatase TiO_2 is more stable when the TiO_2 size is less than 15 nm such as nanoparticles and nanotubes.

However, for nanosize anatase TiO_2, the separated electrons and holes are easily recombined, too, due to higher defect density at the interfaces.[4, 15, 16] The recombination reduces photocatalytic activity of TiO_2. To increase the photocatalytic activity, the nanosize TiO_2 such as TiO_2 nanotubes can be deposited with noble metal nanoparticles.[4, 15–19] Among the various noble metals, Ag is one of the most promising metals, because Ag nanoparticles can act as electron trappers, facilitating electron–hole separation and promote interfacial electron transfer process. Thus, the Ag nanoparticles can slow the rate of electrons and holes recombination on the surface of TiO_2. In addition, Ag nanoparticles can easily fabricated by a photochemical deposition method under UV light irradiation.[19]

These days, as a method in fabricating nanostructures, block copolymer (BCP) lithography which could replace conventional photolithography, has been widely investigated as the nanolithography of various applications such as next generation semiconductors, information storage, photonic crystals, etc.[20–24] A BCP material consists of two or more polymeric chains joined by a covalent bond, which is chemically different and attached each other. BCP materials can self-assemble into uniformly ordered nanostructures such as cylindrical, lamellar, spherical, and gyroid morphologies by phase separation because of connectivity constraints and the incompatibility between the two blocks. Differently ordered nanostructures can be fabricated by varying the volume fraction of the two blocks. The lithography using block copolymer thin films as templates has emerged as a promising low cost and high throughput technology. One of the most common block copolymers, polystyrene–block-polymethylmethacrylate (PS–*b*-PMMA) allows selective removal of PMMA domains by wet and dry methods, and remaining PS domains can serve as the mask for pattern transfer.

There are many methods in fabricating nanosize TiO_2, and among these, TiO_2 nanotubes can have higher surface to volume ratio, therefore, higher photocatalytic properties can be expected. In this study, we fabricated uniform TiO_2 nanotubes with 40 nm scale diameter using a self-aligned, hole patterned BCP template lithography, atomic layer deposition of TiO_2, and reactive ion etching (RIE). In addition, we deposited the Ag nanoparticles onto TiO_2 nanotubes using a photochemical deposition method under UV light irradiation. Then, we compared the photocatalytic degradation of methylene blue (MB) dye solution containing TiO_2 and Ag/TiO_2 nanotubes under UV light irradiation to evaluate the photocatalytic effects. The results showed that the photocatalytic effect of Ag/TiO_2 nanotubes was higher than that of TiO_2 nanotubes without Ag nanoparticles demonstrating the Ag nanoparticles on TiO_2 nanotubes as enhanced photocatalysts.

2. EXPERIMENTAL DETAILS

2.1. Formation of BCP Lithographic Hole Array Pattern on Silicon Substrates

In order to form a PS hole array pattern of 40 nm diameter on silicon substrates, first, the silicon substrates were cleaned with acetone, alcohol, and deionized water. Then, a PS–*b*-PMMA solution composed of 140 kg/mol PS and 65 kg/mol PMMA dissolved in toluene was spin-coated on the cleaned silicon substrates and annealed at 230 °C for 40 h in a vacuum chamber for the phase separation of PS and PMMA. After the thermal annealing, 40 nm diameter cylinder array of PMMA was formed in the PS matrix. The PMMA cylinders in PS matrix were selectively removed by an O_2 plasma at room temperature. As a result, a PS hole array pattern of 40 nm diameter and 60 nm height was formed in the silicon substrates. This PS hole array pattern on silicon substrates was used as the lithographic mask for pattern transfer process.

2.2. Fabrication of Ag/TiO_2 Nanotubes

The silicon substrates with the PS hole array mask pattern were etched by a reactive ion etch (RIE) system. The etching process was carried out with 13.56 MHz 50 W power,

45 sccm of SF_6, and 6.5 mTorr of operating pressure for 45 sec. During the etching process, the main chamber's temperature was maintained at room temperature with a chiller because the PS mask was soft and can be easily collapsed at high temperatures. After the silicon etching, the PS mask was selectively removed by the etcher with 13.56 MHz 50 W power, 50 sccm O_2, and 5 mTorr of operating pressure for 1 min to expose 40 nm diameter uniform silicon hole array pattern. Next, 12 nm thick TiO_2 was uniformly deposited on the silicon hole array pattern by atomic layer deposition (ALD) system (SNTEK, SN 13–20, Korea) using the precursors of titanium isopropoxide (TTIP 97%, Sigma-Aldrich Inc., USA) and O_2. In this process, the growth rate of TiO_2 was about 1.36 Å/cycles at 200 °C. When the structure of deposited TiO_2 was investigated by X-ray diffraction, anatase TiO_2 could be identified for ALD TiO_2 thicker than ~100 nm (for 12 nm thick ALD deposited TiO_2, possibly due to the too thin thickness, the phase of the deposited TiO_2 could not be identified). The top and bottom regions (not the sidewall region of the silicon hole array) of the deposited TiO_2 on the silicon hole array pattern were selectively etched by using the RIE system at 13.56 MHz 50 W bias power, 30 sccm Ar, 20 sccm C_2F_6, and 8 mTorr of operating pressure for 1 min 30 sec. After that, the remained silicon attached to TiO_2 nanotubes was also selectively removed by RIE with 13.56 MHz 50 W bias power, 25 sccm SF_6, and 6.5 mTorr of operating pressure for 45 sec to expose TiO_2 nanotubes (TiO_2 remaining on the sidewall of silicon hole array) from the silicon substrates.

On the uniformly fabricated TiO_2 nanotube array, a photochemical Ag deposition process was carried out. First, the TiO_2 nanotube array samples were immersed in a petri dish filled with 1 mM $AgNO_3$ aqueous solution and sonicated for 30 min. Next, the TiO_2 nanotube array samples in the $AgNO_3$ (silver nitrate, 99.8%, Daejung Inc., Korea) aqueous solution were irradiated with a 12 W UV lamp. The UV irradiation time was varied from 10 to 30 min. After the photochemical process, the samples were washed by deionized water and dried out in an oven at 25 °C for 2 h.

2.3. Characterization

A scanning electron microscopy (FE-SEM, Hitachi, S-4700, Japan) was used to observe the top, cross-sectional, and tilt views of the PS hole array mask pattern, TiO_2 nanotubes, and Ag/TiO_2 nanotubes. X-ray photoelectron spectroscopy (XPS, Thermo, ESCALAB250, England) was used to analyze the surface binding states of the TiO_2 nanostructures deposited by ALD and Ag/TiO_2 nanotubes. For the photolysis test of a dye material, methylene blue was used. Various TiO_2 and Ag/TiO_2 nanostructure samples were immersed in the petri dishes filled with 5ppm methlylene blue ($C_{16}H_{18}ClN_3S$, Junsei Chemical, Japan) aqueous solution and were covered with quartz plates. Then, in dark condition, the samples were irradiated with a 100 W UV lamp emitting a wavelength of 254 nm. A UV-visible spectrophotometer (UV/Vis spectrophotometer, Libra, S2, Biochrom, USA) was used for the measurement of periodical absorbance of the methylene blue aqueous solution at the wavelength of 660 nm.

3. RESULTS AND DISCUSSION

Figure 2 shows cross-sectional, top, and tilted SEM images of (a and b) the PS hole array mask pattern formed by BCP lithography on silicon substrates and (c and d) the silicon hole array after etching the silicon with the PS mask and after the PS mask was removed. As shown in Figures 2(a and b), after the BCP phase separation of PS and PMMA, due to the self-assembly, 60 nm height and 40 nm diameter PS hole array mask pattern was formed by the BCP lithography on silicon substrates. As shown in Figures 2(c and d), after the etching of silicon using the PS hole array mask followed by the removal of the PS mask 60 nm depth and 40 nm diameter uniform silicon hole array with the aspect ratio of 1.5 could be fabricated.

To obtain TiO_2 nanotubes, 12 nm thick TiO_2 was deposited on the 40 nm diameter/60 nm height silicon hole array by ALD using titanium isopropoxide and oxygen as precursors. The TiO_2 growth rate was about 1.36 Å/cycle at 200 °C. Figures 3(a and b) show the cross-sectional and tilted SEM images of TiO_2 deposited on silicon hole array by the ALD, respectively. As shown in Figures 3(a and b), uniform TiO_2 with the thickness of about 12 nm was deposited on the all over the silicon surfaces including the silicon hole area. But, as shown in Figures 3(a and b), the silicon hole was not fully filled with TiO_2 leaving a narrow hole in the silicon hole pattern.

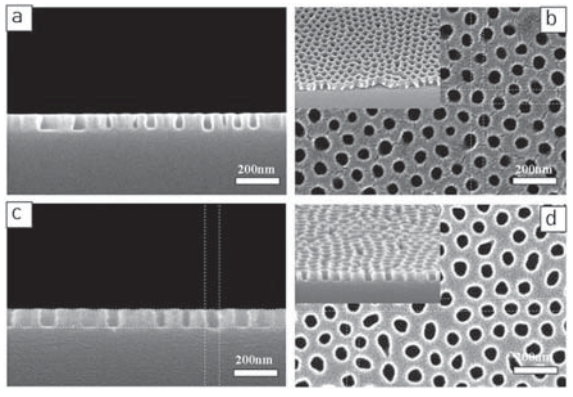

Fig. 2. SEM images of (a) cross-section view and (b) top view of the 60 nm height and 40 nm diameter of the PS hole array mask pattern formed by BCP lithography on silicon substrate. (c and d) are the SEM images of cross-section view and top view of silicon hole array after etching silicon with the PS mask, respectively. After the silicon etching, the silicon hole size was 40 nm and the etch depth was 60 nm. The insets in (b and d) show the SEM images of tilted view of PS hole array mask pattern and etched silicon hole array, respectively.

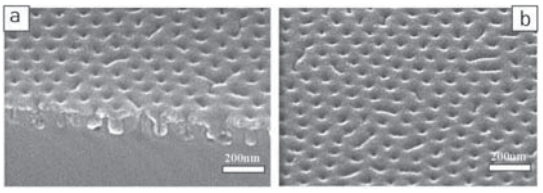

Fig. 3. (a) Cross-sectional and (b) tilted SEM images of TiO_2 deposited on silicon hole array by ALD with titanium isopropoxide and O_2 precursors. The TiO_2 growth rate was about 1.36 Å/cycle at 200 °C and the TiO_2 thickness was about 12 nm.

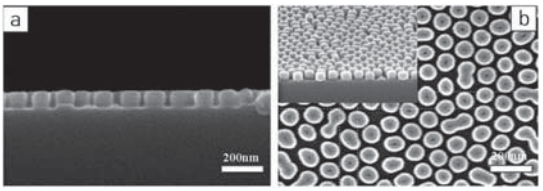

Fig. 4. SEM images (a) cross-sectional, (b) top, and inset of (b) tilted views of fabricated TiO_2 nanotubes.

To form TiO_2 nanotubes, TiO_2 in the top and bottom areas of silicon hole array was selectively etched, therefore, only TiO_2 was remaining on the sidewall of the silicon hole array. After that, the silicon attached with sidewall TiO_2 was selectively removed to obtain TiO_2 nanotubes. Figure 4 shows SEM images (a: cross-sectional, b: top, and inset of (b): tilted views) of fabricated TiO_2 nanotubes. As shown in the figure, after the silicon removal, 50∼60 nm height and 40∼50 nm diameter TiO_2 nanotubes could be obtained on the silicon substrate.

On the fabricated TiO_2 nanotubes, to investigate the effect of Ag nanoparticles attached on the TiO_2 nanotubes, TiO_2 nanotubes were immersed in a 1 mM $AgNO_3$ solution and were irradiated with 12 W UV light for 10∼30 min for the nucleation of Ag nanoparticles on TiO_2 nanotube surfaces. Figure 5 shows the SEM images of

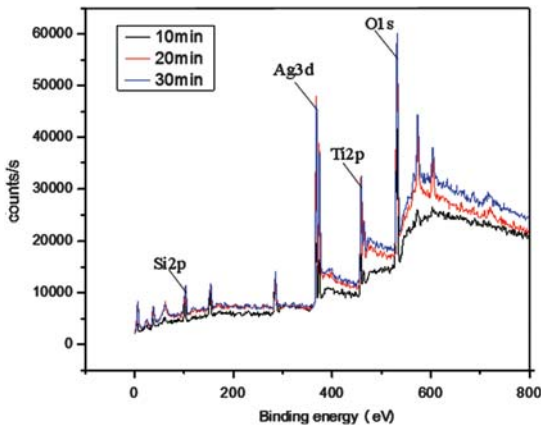

Fig. 6. XPS wide scan data of TiO_2 nanotubes deposited with Ag nanoparticles for 10, 20, and 30 min.

TiO_2 nanotubes deposited with Ag nanoparticles by the immersion in the 1 mM $AgNO_3$ solution while irradiating with 12 W UV light for (a, b) 10 min, (c, d) 20 min, and (e, f) 30 min. As shown in Figure 5, the precipitation of Ag nanoparticles on the TiO_2 nanotube surface could be observed by the immersion in the $AgNO_3$ solution and, with the increase of immersion time, the number of Ag nanoparticles on the TiO_2 surfaces was increased. The measured size of the Ag nanoparticles was in the range from 7 to 9 nm. For the further identification of the formation of Ag nanoparticles on TiO_2 nanotubes after the immersion in the $AgNO_3$ solution, XPS wide scan data were observed for the TiO_2 nanotubes immersed in the $AgNO_3$ solution while irradiating with 12 W UV light for 10∼30 min and the results are shown in Figure 6. As shown in Figure 6, with the increase of UV irradiation time, the increased Ag peak intensities were observed indicating the increased number of Ag nanoparticles.

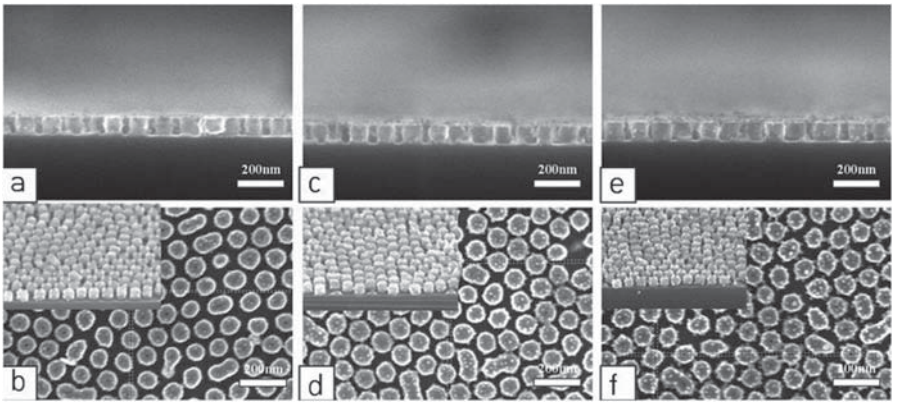

Fig. 5. SEM images (cross-sectional, top, and tilted views) of Ag deposited TiO_2 nanotubes using a photochemical deposition method. To deposit Ag nanoparticles, TiO_2 nanotubes were immersed in a 1 mM $AgNO_3$ solution and were irradiated with 12 W UV light for (a, b) 10 min, (c, d) 20 min, and (e, f) 30 min. The average size of formed Ag nanoparticles was about 7∼9 nm.

Using the TiO_2 nanotubes with and without Ag nanoparticles, the photocatalytic properties were investigated. For the photocatalytic properties, the samples were immersed in a 5 ppm, 15 ml methylene blue aqueous solution and irradiated with a 100 W UV lamp emitting a wavelength of 254 nm up to 3 hours. The change of concentration by the decomposition of the methylene blue solution was measured by measuring the change of light absorption at 660 nm, which is the peak absorption wavelength of the methylene blue, using a UV-visible spectrometer. Figure 7 shows the change in the concentration of the methylene blue aqueous solution for various TiO_2 samples. As references, the changes of the concentration with the UV radiation for the methylene blue aqueous solution without TiO_2 and for the 12 nm thick TiO_2 thin film deposited on flat silicon substrate were included in addition to the concentration changes for the TiO_2 nanotubes and TiO_2 nanotubes deposited with Ag nanoparticles for 10, 20, and 30 min. As shown in Figure 7, no noticeable change of concentration was observed for the methylene blue solution without TiO_2 while the solution with 12 nm TiO_2 flat thin film showed about 2% of concentration change after 3 h. The solution with the TiO_2 nanotubes exhibited higher concentration change of the methylene blue solution possibly due to the increased surface area. The TiO_2 nanotubes with Ag nanoparticles exhibited the higher concentration change compared to TiO_2 nanotubes alone by facilitating electron–hole separation and promoting interfacial electron transfer process through the Ag nanoparticles. Among the TiO_2 nanotubes with Ag nanoparticles, the Ag nanoparticles deposited for 20 min exhibited the most prominent photocatalytic effect among the TiO_2 with Ag nanoparticles by reducing the concentration of the methylene blue aqueous solution about 8% after 3 h of UV radiation.

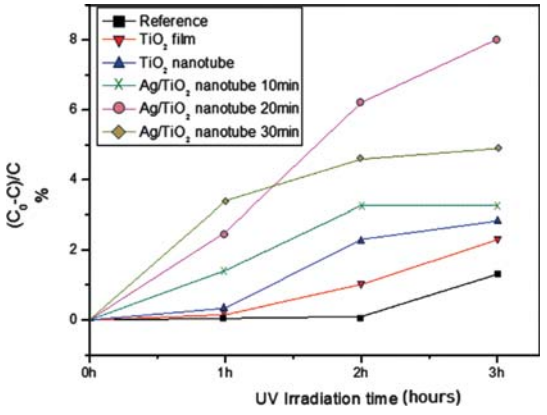

Fig. 7. Change in the concentration of a 5 ppm methylene blue aqueous solution with 100 W UV light for various TiO_2 samples. As references, the change of the concentration with UV radiation for the methylene blue aqueous solution without TiO_2 and for the 12 nm thick TiO_2 thin film deposited on flat silicon substrate were included in addition to the TiO_2 nanotubes and TiO_2 nanotubes deposited with Ag nanoparticles for 10, 20, and 30 min.

The lower photocatalytic effect for the TiO_2 deposited with Ag nanoparticles for 30 min appears to be related to the decreased UV penetration to TiO_2 by the increased surface area covered with Ag nanoparticles.

4. CONCLUSION

Using the TiO_2 nanotubes fabricated with BCP lithography, TiO_2 ALD, and etching and Ag nanoparticles precipitated on TiO_2 nanotubes by a photochemical method, the photocatalytic effect of TiO_2 nanotubes with/without Ag nanoparticles was investigated by measuring the concentration change of a methylene blue solution. The photocatalytic effect of TiO_2 nanotubes was higher than flat TiO_2 film because of the increased TiO_2 surface area. Also, Ag nanoparticles attached on the TiO_2 nanotubes further improved the photocatalytic effect by facilitating electron–hole separation and promoting interfacial electron transfer process through the Ag nanoparticles. However, when the amount of Ag nanoparticles on TiO_2 nanotubes are too much, possibly due to the decreased UV penetration to TiO_2 by the increased surface area covered with Ag nanoparticles, the photocatalytic effect was decreased. By precipitating 7∼9 nm size Ag nanoparticles for 20 min on 40∼50 nm diameter/50∼60 nm height TiO_2 nanotubes, the highest photocatalytic effect could be obtained.

Acknowledgment: This research was supported by Nano-Material Technology Development Program through the National Research Foundation of Korea (NRF) funded by the Ministry of Education, Science and Technology (2012M3A7B4035324). And it was supported by the NRF (National Research Foundation of Korea (2016M3A7B4910429)).

References and Notes

1. A. Word, *Chem. Mater.* 5, 280 (**1993**).
2. D. Wang, Z. H Zhou, H. Yang, K. B. Shen, Y. Huang, and S. Shen, *R. Soc.* 22, 16306 (**2012**).
3. R. Liu, P. Wang, X. Wang, H. Yu, and J. Yu, *Phys. Chem. B* 116, 17721 (**2012**).
4. H. M. Sung-Suh, J. R. Choi, H. J. Hah, S. M. Koo, and Y. C. Bae, *J. Photochem. Photobiol. A* 163, 37 (**2003**).
5. M. Paulose, K. Shankar, O. K. Varghese, G. K. Mor, and C. A. Grimes, *J. Phys. D: Appl. Phys.* 39, 2498 (**2006**).
6. J. Keleher, J. Bashant, N. Heldt, L. Johnson, and Y. Li, *World J. Microbiol. Biotechnol.* 18, 133 (**2002**).
7. Y. Lai, H. Zhuang, K. Xie, D. Gong, Y. Tang, L. Sun, C. Lin, and Z. Chen, *New J. Chem.* 34, 1335 (**2010**).
8. J. M. Macak, H. Tsuchiya, A. Ghicov, K. Yasuda, R. Hahn, S. Bauer, and P. Schmuki, *Curr. Opin. Solid State Mater. Sci.* 11, 3 (**2007**).
9. Y. Liao, H. Zhang, Z. Zhong, L. Jia, F. Bai, J. Li, P. Zhong, H. Chen, and J. Zhang, *ACS Appl. Mater. Inter.* 5, 11022 (**2013**).
10. J. Schneider, M. Matsuoka, M. Takeuchi, J. Zhang, Y. Horiuchi, M. Anpo, and D. W. Bahnemann, *Chem. Rev.* 114, 9919 (**2014**).
11. C. H. Wu and J. M. Chern, *Ind. Eng. Chem. Res.* 45, 6450 (**2006**).
12. I. K. Konstantinou and T. A. Albanis, *Appl. Catal. B-Environ.* 49, 1 (**2004**).
13. D. O. Scanlon, C. W. Dunnill, J. Buckeridge, S. A. Shevlin, A. J. Logsdail, S. M. Woodley, C. R. A. Catlow, M. J. Powell, R. G.

Palgrave, I. P. Parkin, G. W. Watson, T. W. Keal, P. Sherwood, A. Walsh, and A. Sokol, *Nat. Mater.* 12, 798 **(2013)**.
14. K. Woan, G. Pyrgiotakis, and W. Sigmund, *Adv. Mater.* 21, 2233 **(2009)**.
15. T. T. Y. Tan, C. K. Yip, D. Beydoun, and R. Amal, *Chem. Eng. J.* 95, 179 **(2003)**.
16. Y. C. Liang, C. C. Wang, C. C. Kei, Y. C. Hsueh, W. H. Cho, and T. P. Perng, *J. Phys. Chem. C* 115, 9498 **(2011)**.
17. I. Paramasivam, J. M. Macak, A. Ghicov, and P. Schmuki, *Chem. Phys. Lett.* 445, 223 **(2007)**.
18. L. Miao, Y. Ina, S. Tanemura, T. Jiang, M. Tanemura, K. Kaneko, S. Toh, and Y. Mori, *Surf. Sci.* 601, 2792 **(2007)**.
19. Y. Ohko, T. Tatsuma, T. Fujii, K. NaoI, C. Niwa, Y. Kumota, and A. Fujishima, *Nat. Mater.* 2, 29 **(2003)**.
20. Z. Liu, X. Gu, J. Hwu, S. Sassolini, and D. L. Olynick, *Nanotechnology* 25, 285301 **(2014)**.
21. S. W. Choi, J. H. Shin, M. H. Jeon, J. H. Mun, S. O. Kim, G. Y. Yeom, and K. N. Kim, *J. Nanosci. Nanotechnol.* 15, 8093 **(2015)**.
22. J. Y. Cheng, C. A. Ross, E. L. Thomas, H. I. Smith, and G. J. Vancso, *Appl. Phys. Lett.* 81, 3657 **(2002)**.
23. X. Gu, Z. Liu, I. Gunkel, S. T. Chourou, S. W. Hong , D. L. Olynick, and T. P. Russell, *Adv. Mater.* 24, 5688 **(2012)**.
24. S. O. Kim, H. H. Solak, M. P. Stoykovich, N. J. Ferrier, J. J. D. Pablo, and P. F. Nealey, *Nature* 424, 411 **(2003)**.

Received: 17 February 2016. Accepted: 15 September 2016.